Egypt. J. Chem. **Vol. 64,** No. 7 pp. 3289 - 3296 (2021)

Egyptian Journal of Chemistry

http://ejchem.journals.ekb.eg/

Investigation of the Influence of Membrane Type on the Performance of Microbial Fuel Cell

Hayder A. Waheeb [a]*, Ahmed Faiq Al-Alalawy [b]

[a,b]*Department of Chemical Engineering, College of Engineering, University of Baghdad, Baghdad, Iraq*

Abstract

In this work, microbial fuel cell (MFC) design of five chambers was used to investigate the effect of four types of membranes which are cation exchange membrane (CEM), Cellulose Triacetate membrane (CTA), thin film composite membrane (TFC), and proton exchange membrane (PEM). To study the influence of the membrane type on the cathode performance, the four cathode chambers were filled with 20 g/l NaCl catholyte and the sodium acetate of 1.5 g/l was supplied to the central chamber as anolyte. The results revealed that the membrane proton selectivity plays an important role in the cathodic reduction reaction for electrical generation and water production. It was observed that the PEM has a significant effect on the power generation with a maximum power density of 20.492 mW/m^2 with water production of 4.21 g/day. Whereas the competition of the other cations to the proton transfer was clearly observed by using the CTA membrane with power production of 12.646 mW/m^2, and the abundance of the water production of 178.16 g/day was attributed to the water transport across the CTA membrane. For studying the influence of the membrane type on the anode performance, the sodium acetate of 1.5 g/l was supplied to the four chambers as an anolyte at a flow rate of 0.0272 cm^3/sec and the central chamber were filled with 20 g/l NaCl catholyte. The salt reverse transfer from the cathode chamber to the anode chamber across the CTA membrane contributed to increasing the anolyte electrical conductivity and consequently increased the power production to 12.555 mW/m^2. Meanwhile, the effect of the proton selectivity and the electrical resistance of the other membrane were observed in the other chambers. Thus, the usage of CEM, TFC, and PEM produced electrical power of 6.751, 3.004, and 9.712 mW/m^2 respectively.

Keywords: Microbial Fuel Cell; Membrane; Power Density.

1. Introduction

Massively, The human population increases [1] leading the world to face two crucial crises which are; i) rapid worldwide increase in energy demand [2,3] which created an energy crisis represented by the depletion of fossil fuels due the high energy consumption [4,5,6] combined with the environmental pollution due to the atmospheric emissions of the greenhouse gases, contributing the global warming and acidification of the surface water [5,7], ii) Water scarcity; the water suitable for human consumption is only 2.5% [3,7], which is currently suffered due to increasing pollution and discharging wastewater [8]. Whereas, the other 97% of water is seawater and brackish water that could be usable after effective desalination [3,9,1].

A typical bio-electrochemical systems (BESs) are capable to alleviate energy consumption and resource recovery crises [10,11,7,12,3,13,14] (such as microbial fuel cells (MFCs) for electricity generation, microbial desalination cells (MDCs) for brackish water desalination, and microbial electrolysis cells (MECs) for hydrogen production) [10]. The microbial fuel cell (MFC) is a device that utilizes microorganisms as a catalyst to directly transform the organic matter chemical energy that existed in wastewater into electrical energy [15,5,16]. MFCs have been designed in many configurations and constructed from various materials [17]. A typical MFC is composed mainly of two-compartment (anode and cathode compartments) that separated by a proton or a cation exchange membrane or salt bridge [18]. MFC functions as a bio-electrochemical process in three sequential steps [16]. Firstly, in the anode chamber, the oxidizable substrate materials by the microorganisms produce an electron and proton [2,19]. Secondly, electrons may transfer from microorganisms to the anode surface by one of the following ways; directly membrane mediates to electron transfer, the employment of mobile shuttle

*Corresponding author e-mail: hayder.waheeb@yahoo.com.; (Hayder A. Waheeb).
Receive Date: 13 January 2021, Revise Date: 03 March 2021, Accept Date: 18 March 2021
DOI: 10.21608/EJCHEM.2021.57995.3247

mediated to electron transfer, or the microorganism's usage of conductive pili to electron transfer [17]. Finally, the electrons transfer from the anode to the cathode electrode through the external electric circuit generating electrical power [20,21]. Thirdly, the protons and the electrons react together at the cathode electrode and reduce the oxidant as the final electron acceptor (usually the atmospheric oxygen) that dissolves in the catholyte completing the electrical circuit and producing water [19,21,22,23].

As the MFC is a sustainable and inexpensive technology, that tempting of applying it in many ways such as [24,25] wastewater treatment by breaking down the chemicals to remove the organic matter, nitrogen [26], and heavy metals [7], electricity generation due to electron flow through the electrical circuit [23,16,27,26], recovery of valuable products like biohydrogen [28] and metals using biocathodes such as Cr(VI) and Co(II) [23], biosensors to analyses pollutants and in-situ process monetarize and control [18], and pretreatment of desalination processes [7] to alleviate salts and dissolved solids [1].

The primary challenges in the MFC field are the design and scaling up of a compact bio-electrochemical reactor that utilizes available and inexpensive material to obtain a good MFC performance and convenient to operate and maintained under conditions of continuous flow [29]. The MFC implementation hinders by many limitations [16] that generally associated with the anode, cathode compartments [4], and the separating membrane [30]. At the anode chamber, the researchers determined the main limitations of the MFC performance such as substrate diffusion [30] and oxidation [31], electron transfer from microorganism to the anode surface, circuit resistance [31], and protons diffusion to the anolyte [30]. While, oxygen reduction reaction, cathodic overpotential, and the catholyte sustainability are the major electrochemical limitations of MFC performance at the cathode chamber [16]. The employment of membranes is a crucial limiting factor to apply the MFC for wastewater treatment and power production [30,31] due to crossover oxygen and substrate [32], membrane resistance [17], membrane fouling [30], proton transfer, and membrane materials high cost [30,31].

Membrane structural materials have an important role to develop the MFC performance due to practical implementation and cost-effectiveness [33]. Several studies are ongoing for the investigation to combine materials of multi-functional, high performance, and inexpensive cost to establish an easy and economical MFC performance [34]. In general, researches focused on materials that are strong and porous with high chemical stability that allow to implementation of anode and cathode electrodes close together and prevent the diffusion of oxygen and substrate [33,34].

Qin et al. (2017) observed that the internal resistance could be reduced by using forward osmosis membrane (FO) and enhanced water recovery in the osmotic microbial fuel cell (OMFCs) by the permeating water under the osmotic pressure gradient from high water potential to low water potential [35,36,37,38] with less permeability to oxygen and substrate [36,39] leading to protons and cations reaches the cathode electrode that electro-osmotically dragged by water molecules in a faster way [40].

In the OsMFC operation, the catholyte plays the key role as the draw solution with high electrical conductivity and robust buffer capacity serving water flux and electricity production [39]. OMFCs face some of the forward osmosis restrictive drawbacks such as reverse salt flux (RSF) which is the backward transport of solute into anolyte chamber due to solute concentration gradient across the membrane [39,41] resulting in decreasing water flux, contaminating the anolyte, and loss of draw solutes [39].

In the previous study, Waheeb and Al-Alalawy (2020) designed the five chambers microbial fuel cell to study the cathodic operation factors of the four chambers that surrounding the central anode. In this cell, the cathode electrode surface area was 156-936 cm^2, the cathode electrode distance from the membrane was 3-9 cm, three types of electrolytes of Na_2SO_4, KCl, and NaCl were used at 50 mM, and using dissolved ozone for electrical generation enhancement. It was found that the electrical power generation increased with increasing the electrode surface area and decreasing the distance from the membrane which was 23.051 mW/m^2 at 936 cm^2 and 9.303 mW/m^2 at distance of 3 cm. While, the Na_2SO_4 catholyte produced the higher power density (3.068 mW/m^2) due to the higher catholyte electrical conductivity (9.14 mS/cm). Whereas, the electrical power generation by using dissolved ozone was about 15 times higher than by using dissolved oxygen [42].

In this study, the microbial cell of five chambers design will be used to study the effect of the membrane types (CEM, CTA, TFC, and PEM) on the cathodes and anodes chambers separately (electrical power generation, water production, and chemical oxygen demand (COD) removal efficiency). For the cathode side, the effect of membranes on proton transfer and water production was studied. While for the anode side, the effect of these membranes on the reverse salt flux and the COD removal efficiency was studied.

2. Experimental Work

2.1. MFC Setup

The novel design of five chambers MFC that developed in our previous research was used, which

was made by Plexiglas materials [42]. The MFC was configured of one central chamber surrounded by four equally sized chambers. The dimensions of the central chamber were 18×18×14 cm and surrounded by four chambers with dimensions of 14×14×14 cm separated from the central chamber by a membrane. The central graphite electrode was designed as a cylinder, an outside diameter of 12 cm. That electrode pierced at the center with a diameter of 8 cm in the depth of 10 cm. Whereas, one flat plate graphite electrode with dimensions of 12×13×0.3 cm was installed at a distance of 3 cm from the membrane in each chamber of the other four compartments (see Fig. 1. a and b). This design permitted to investigate the effect of the applied load between the anode and the cathode electrodes and the membrane type on the electricity generation and water production with the neutralization of operational conditions in the central chamber for the other chambers.

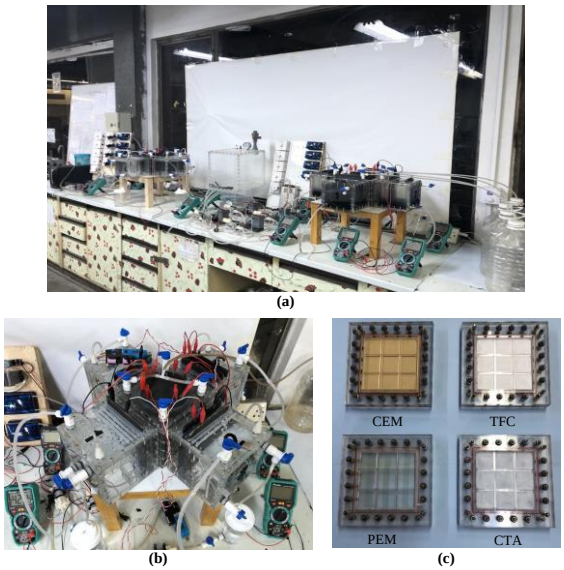

Fig. 1 (a) The microbial fuel cell, (b) The five-chambers design, and (c) Types of membranes.

Four types of membrane were utilized which are cation exchange membrane (CEM) - CMI 7000 (Membrane International INC., NJ, USA), Cellulose Triacetate (CTA) (Sterlitech, Kent, Washington, USA), Thin Film Composite TFC (Koria), and proton exchange membrane - Nafion 117 (The Fuel Cell Store, Texas, USA), where the active layers were faced the anode chamber (see Fig. 1. c).

2.2. MFC Startup

The anode chamber was inoculated with the active sludge that composite of a mixture of bacteria (Pseudomonas bacterial in most). To achieve anaerobic conditions, the anode chamber and feeding tank was flashed with nitrogen gas for a period more than 30 min. The anode chamber was fed continuously from the bottom of the chamber with oxygen-free simulated wastewater composed from 1.5 g/l of sodium acetate dissolved in distilled water as an organic waste source. Four peristaltic pumps that locally assembled were used to supply the anode chamber with the simulated wastewater at a specific flowrate 0.0272 cm^3/sec to achieve 28h as a hydraulic retention time (HRT).

The central chamber was applied as the anode chamber and the four surrounding chambers as the cathode chambers each one was pumped with air at 100 cm^3/min to ensure saturated dissolved oxygen condition for improving the cathodic oxygen reduction reaction in order to study the effect of the membrane type on the cathode chamber conditions (i.e., electrical generation and water production). All cathode chambers were filled with a sodium chloride solution at a concentration of 20 g/l as a catholyte solution, which was refreshed every day from an external tank. Whereas, the central chamber as the cathode chamber was supplied with air at volumetric flow rate 400 cm^3/min by four air pumps to ensure saturated dissolved oxygen condition improving the cathodic oxygen reduction reaction. The four surrounding chambers as the anode chambers were utilized to study the effect of the membrane type on the anode chamber conditions (i.e., electrical generation and COD removal).

2.3. Measurement and analysis

The measurements of Chemical oxygen demand (COD) for the wastewater were carried out by using Thermo-reactor RD 125 (Lovibond, Germany), where the aqueous samples were heated for two hours at 150 ˚C and chemically digested. Then, the value of COD was determined by MD 200 COD Photometer (Lovibond, Germany) and the COD removal efficiency was calculated by

$$\eta_{COD} = \frac{COD_{in} - COD_{out}}{COD_{in}} \times 100 \qquad (1)$$

The total dissolved solids (TDS), solution conductivity (k), and pH were tested by portable tester (HANA, Romania).

The produced voltage and current between the anode and cathode for each chamber were measured by a digital multimeter (ProsKit MT-1707, Taiwan). To perform the polarization curve, the external resistance which represented the load between the anode and cathode was varied in the range of 0-10000 Ω through a resistance box, and the data was recorded ten minutes later after changing the external

resistance. The current density (mA.cm^{-2}) was calculated by $I = i/A$, and the power density (mW/cm^2) was calculated by $P = IV$, where i is the generated current, A (mA) the anode surface area (cm^2), V the voltage between the anode and cathode (mV). A digital balance was used to measure the water production

3. Results and Discussions

In this research, the polarization curves and the startup output voltage and current have been measured and the polarization curves for each anode and cathode were calculated to investigate the effect of the membrane type on the power density. The effect of the membrane types on the MFC performance was studied by implementing the cation exchange membrane (CEM), the Cellulose Triacetate (CTA), the Thin Film Composite (TFC), and the proton exchange membrane (PEM) between the anode and cathode chambers. A resistance of 1 kΩ as an electrical load was installed between the anode electrode and each cathode electrode.

3.1. The cathode performance

The results showed that the water productions were 2.06 g/day then decreased to 0.26 g/day on the 4th day for CEM, 178.16 g/day then decreased to 84.27 g/day which continued to the 28th day for CTA, and 4.21 g/day reduced to 0.12 g/day on the 9th day for PEM. Meanwhile, there was no water production in the 3rd chamber. As shown in Fig. 2, the water production was evident in the 2nd chamber due to the water production by the cathodic reaction reduction and the significant water transfer through the Cellulose Triacetate from the higher water potential at the anode chamber to the lower water potential at the cathode. Whereas, the water production was not significant in the other cathode chambers due to diminished water transfer through the other membranes and the effect of the water evaporation by air pumping. The decrease in water production may be attributed to the fouling on the membrane in the anode side.

At the steady state, the results show that the startup voltages were 270.5, 284.9, 241.9, and 314.7 mV for the utilization of the CEM, CTA, TFC, and PEM respectively (see Fig. 3). Also, the startup currents were 0.241, 0.254, 0.218, and 0.285 mA for the utilization of the CEM, CTA, TFC, and PEM respectively. Figures 3 and 4 revealed that the startup voltage and current flow through the resistance of 1 kΩ for each cathode electrode had the same pattern of the generated power density by using the four different membranes, which indicates that this pattern is due to the effect of bacterial activity with the anode electrode.

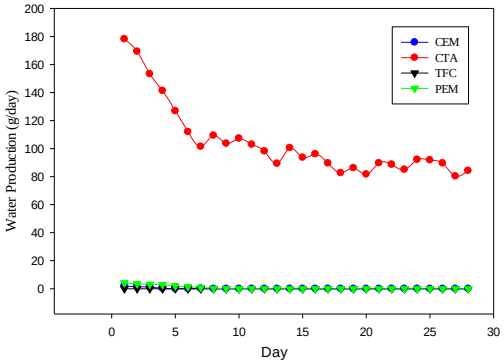

Fig. 2. The measured water production in each cathode chamber.

While, the increase of the cell voltage and current with time was attributed to the biofilm growth on the anode electrode.

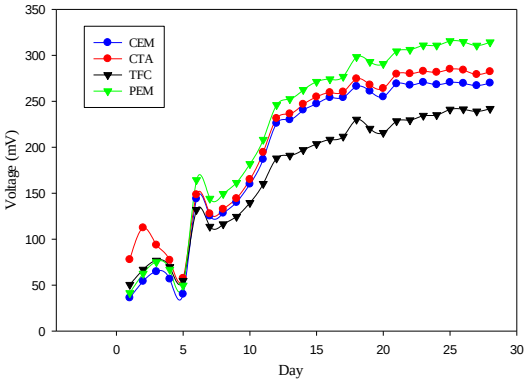

Fig. 3. The measured startup voltage for each cathode chamber.

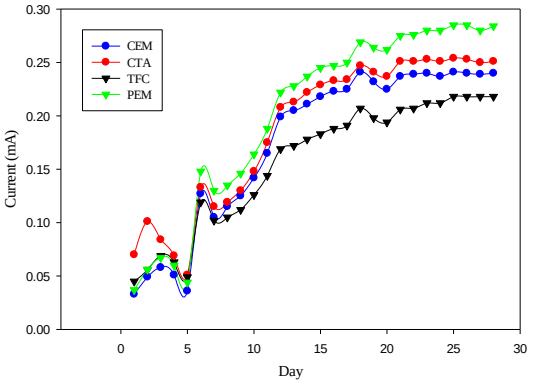

Fig. 4. The measured startup current for each cathode chamber.

For the close circuit performance, the higher generated power densities were 5.025, 12.646, 3.901, and 20.492 mW/m^2 for CEM, CTA, TFC, and PEM

respectively, as shown in Fig. 5. The results revealed that the utilizing of the proton exchange membrane produced the higher electrical power generation due its higher selectivity to proton transfer to the cathode. The abundance of the proton on the cathode surface increasing the cathodic reduction reaction rate, this behavior is agreement with Venkata et al. 2008 [43]. On the other hand, the Cellulose Triacetate CTA, the cation exchange membrane CEM, and the Thin Film Composite TFC allowed proton and other dissolved cations to transfer to the cathode chamber. The absence of the proton transfer selectivity in these membranes permeated to the other cations to competition the protons in the cathodic reduction reaction which leading to decrease the generated power density. This result is in agreement with Qin et al. (2017) [35].

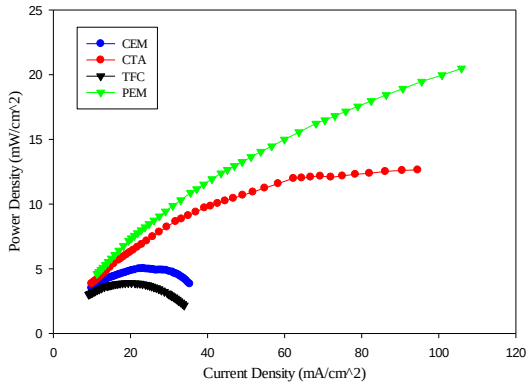

Fig. 5. The polarization curve for each cathode chamber.

The generated power density by using the Cellulose Triacetate was higher than the cation exchange membrane due to the higher proton transfer to the cathode chamber by convection transfer with water, consequently producing higher electrical power density. This result agrees with Qin et al. (2017) [35]. Whereas, the utilization of the Thin Film Composite produced the lower power density because of the higher resistivity to transfer the protons to the cathode chamber. It was remarkable that the usage of the CEM and TFC increased the internal resistance to 340 and 500 Ω respectively.

3.2. The anode performance

Fig. 6 revealed that the reverse salt flux occurred from the cathode chamber to the other anode chambers across each membrane due to salt concentration difference between the anode and cathode chambers. The reverse salt flux for the CTA was higher than the other membranes and decreased for the PEM, CEM, and TFC successively. This behavior is attributed to the difference in the salt permeability for each membrane. For the CTA, the reverse salt flux increased with time until the 13th day, meanwhile, the revers salt transfer for the PEM started to decrease on the 9th day. On the other hand, the decreased reverse salt flux for the CEM and TFC lasted every day to the experiment end.

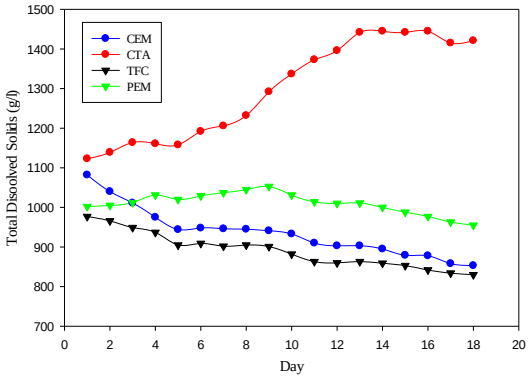

Fig. 6. The measured total dissolved solid in each anode chamber.

The results showed that the anolyte electrical conductivities were 1.74, 2.93, 1.69, and 1.95 mS/cm by the utilizing the CEM, CTA, TFC, and PEM respectively. Fig. 7 demonstrated that the anolyte electrical conductivity by applying the CTA membrane was higher than the other chambers due to higher reverse salt flux across the CTA membrane. Also, it was revealed that the electrical conductivity affected by the reverse salt flux across the membrane in each chamber which agreed with Qin et al. (2016) [39].

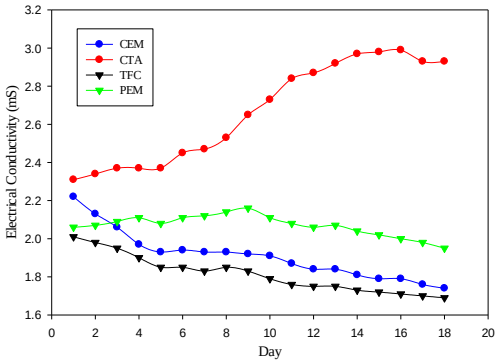

Fig. 7. The measured electrical conductivity in each anode chamber.

The results revealed that the higher COD removal efficiencies were 46.5, 33.9, 48.94, and 45.12% by using CEM, CTA, TFC, and PEM respectively, as

shown in Fig. 8. The COD removal efficiency in the anode chambers is affected by the salt reverse flux. Where the COD removal efficiency decreases with the increase in salt concentration because of the inhibition of the bacterial activity and consequently decreasing the organic matter bioremediation. Thus, it was observed that the higher COD removal efficiency was obtained by the use of TFC, CEM, PEM, and CTA successively. This result agreed with Cao et al. (2010) [44].

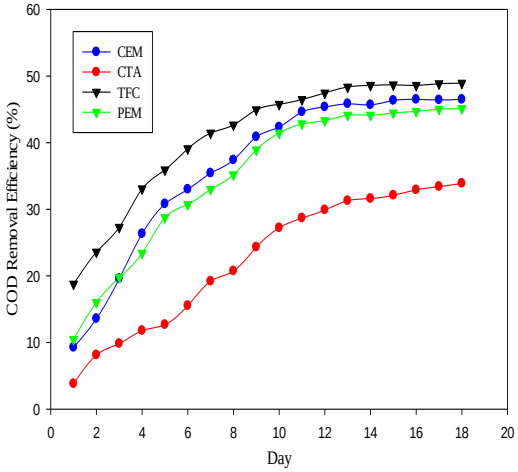

Fig. 8. The COD removal efficiency in each anode chamber.

The results showed that the higher generated power densities were 6.751, 12.555, 3.004, and 9.712 mW/m^2 by using CEM, CTA, TFC, and PEM respectively. Fig. 9 demonstrated that the generated power density increased with the increase in the anolyte electrical conductivity (see Fig. 7) due to the increase in the reverse salt transfer across the membrane as shown in Fig. 6. The use of the CTA produced the higher power density due to higher anolyte electrical conductivity, which increases attributing for two reasons. The first reason, the CTA has the higher reverse salt flux from the catholyte. The second reason, the CTA has the higher water flux from the anode chamber which concentrate the anolyte. Furthermore, the use of the CTA generated more electrical power because of more proton transfer by convection across the membrane. These results were consistent with both Zan et al. (2011) and Vilas et al. (2015) [45,46].

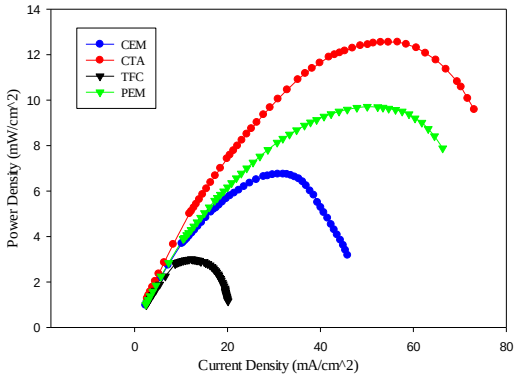

Fig. 9. The polarization curve for each anode chamber.

4. Conclusions

In this work, the usage of the cation exchange membrane (CEM), Cellulose Triacetate membrane (CTA), thin film composite membrane (TFC), and proton exchange membrane (PEM) permitted to generate electrical power. For the central anode performance, the proton selectivity of the PEM allowed to produce the higher power generation (20.492 mW/m^2). Whereas, the CTA membrane produced more water (178.16 g/day). For the central cathode performance, the water transfer and reverse salt flux across the CTA membrane was significantly more than the other membrane. The implementing the CTA membrane resulted in more power generation of (12.555 mW/m^2). The water transfer from the anode to cathode chambers attributed to decrease the COD removal efficiency to 33.9% by implementing the CTA membrane whereas, the use of the TFC increased the COD removal efficiency to the higher value of about 48.94%.

5. References

[1] A. Al-Mamun, W. Ahmad, M. S. Baawain, M. Khadem, and B. R. Dhar, "A review of microbial desalination cell technology: Configurations, optimization and applications," *J. Clean. Prod.*, vol. 183, pp. 458–480, 2018.

[2] R. Patel and D. Deb, "Control-oriented parametrized models for microbial fuel cells," *2017 6th Int. Conf. Comput. Appl. Electr. Eng. - Recent Adv. CERA 2017*, vol. 2018-Janua, no. July, pp. 152–157, 2018.

[3] X. Chen, P. Liang, X. Zhang, and X. Huang, "Bioelectrochemical systems-driven directional ion transport enables low-energy water desalination, pollutant removal, and resource recovery," *Bioresour. Technol.*, vol. 215, pp. 274–284, 2016.

[4] M. Vaez, S. Karami-Rad, S. Tavakkoli, and H. Diba, "Microbial Fuel Cells, Features and Developments," *Curr. World Environ.*, vol. 10, no. Special-Issue1, pp. 637–643, 2015.

[5] Z. Baicha et al., "A critical review on microalgae as an alternative source for bioenergy production: A promising low cost substrate for microbial fuel cells," *Fuel Process. Technol.*, vol. 154, pp. 104–116, 2016.

[6] M. Esfandyari, M. A. Fanaei, R. Gheshlaghi, and M. Akhavan Mahdavi, "Mathematical modeling of two-chamber batch microbial fuel cell with pure culture of Shewanella," *Chem. Eng. Res. Des.*, vol. 117, pp. 34–42, 2017.

[7] E. Yang, K. J. Chae, M. J. Choi, Z. He, and I. S. Kim, "Critical review of bioelectrochemical systems integrated with membrane-based technologies for desalination, energy self-sufficiency, and high-efficiency water and wastewater treatment," *Desalination*, vol. 452, no. October 2018, pp. 40–67, 2019.

[8] B. Zhang and Z. He, "Improving water desalination by hydraulically coupling an osmotic microbial fuel cell with a microbial desalination cell," *J. Memb. Sci.*, vol. 441, pp. 18–24, 2013.

[9] F. L. Moruno, J. E. Rubio, C. Santoro, P. Atanassov, J. M. Cerrato, and C. G. Arges, "Investigation of patterned and non-patterned poly(2,6-dimethyl 1,4-phenylene) oxide based anion exchange membranes for enhanced desalination and power generation in a microbial desalination cell," *Solid State Ionics*, vol. 314, no. November, pp. 141–148, 2018.

[10] X. Chen, D. Sun, X. Zhang, P. Liang, and X. Huang, "Novel Self-driven Microbial Nutrient Recovery Cell with Simultaneous Wastewater Purification," *Sci. Rep.*, vol. 5, no. October, pp. 1–10, 2015.

[11] X. Chen, H. Sun, P. Liang, X. Zhang, and X. Huang, "Optimization of membrane stack configuration in enlarged microbial desalination cells for efficient water desalination," *J. Power Sources*, vol. 324, pp. 79–85, 2016.

[12] Z. Z. Ismail and M. A. Ibrahim, "Desalination of oilfield produced water associated with treatment of domestic wastewater and bioelectricity generation in microbial osmotic fuel cell," *J. Memb. Sci.*, vol. 490, no. September, pp. 247–255, 2015.

[13] P. Pandey, V. N. Shinde, R. L. Deopurkar, S. P. Kale, S. A. Patil, and D. Pant, "Recent advances in the use of different substrates in microbial fuel cells toward wastewater treatment and simultaneous energy recovery," *Appl. Energy*, vol. 168, pp. 706–723, 2016.

[14] D. R. Saad, Z. T. Alismaeel, and A. H. Abbar, "Cobalt Removal from Simulated Wastewaters Using a Novel Flow-by Fixed Bed Bio-electrochemical Reactor," Chem. Eng. Process. - Process Intensif., vol. 156, no. May, p. 108097, 2020.

[15] C. Y. Cheng, C. C. Li, and Y. C. Chung, "Continuous Electricity Generation and Pollutant Removal from Swine Wastewater Using a Single-Chambered Air-Cathode Microbial Fuel Cell," *Adv. Mater. Res.*, vol. 953–954, pp. 158–162, 2014.

[16] Y. Zeng, Y. F. Choo, B. H. Kim, and P. Wu, "Modelling and simulation of two-chamber microbial fuel cell," *J. Power Sources*, vol. 195, no. 1, pp. 79–89, 2010.

[17] B. E. Logan et al., "Microbial fuel cells: Methodology and technology," *Environ. Sci. Technol.*, vol. 40, no. 17, pp. 5181–5192, 2006.

[18] Z. Du, H. Li, and T. Gu, "A state of the art review on microbial fuel cells : A promising technology for wastewater treatment and bioenergy," *Biotechnol. Adv.*, vol. 25, pp. 464–482, 2007.

[19] X. A. Walter, S. Forbes, J. Greenman, and I. A. Ieropoulos, "From single MFC to cascade configuration: The relationship between size, hydraulic retention time and power density," *Sustain. Energy Technol. Assessments*, vol. 14, pp. 74–79, 2016.

[20] A. Al-Mamun, O. Lefebvre, M. S. Baawain, and H. Y. Ng, "A sandwiched denitrifying biocathode in a microbial fuel cell for electricity generation and waste minimization," *Int. J. Environ. Sci. Technol.*, vol. 13, no. 4, pp. 1055–1064, 2016.

[21] Y. Y. Lee, T. G. Kim, and K. S. Cho, "Characterization of the COD removal, electricity generation, and bacterial communities in microbial fuel cells treating molasses wastewater," *J. Environ. Sci. Heal. - Part A Toxic/Hazardous Subst. Environ. Eng.*, vol. 51, no. 13, pp. 1131–1138, 2016.

[22] Z. Li, X. Zhang, Y. Zeng, and L. Lei, "Electricity production by an overflow-type wetted-wall microbial fuel cell," *Bioresour. Technol.*, vol. 100, no. 9, pp. 2551–2555, 2009.

[23] Y. V. Nancharaiah, S. Venkata Mohan, and P. N. L. Lens, "Metals removal and recovery in bioelectrochemical systems: A review," *Bioresour. Technol.*, vol. 195, pp. 102–114, 2015.

[24] A. Al-Mamun, M. S. Baawain, B. R. Dhar, and I. S. Kim, "Improved recovery of bioenergy and osmotic water in an osmotic microbial fuel cell using micro-diffuser assisted marine aerobic biofilm on cathode," *Biochem. Eng. J.*, vol. 128, pp. 235–242, 2017.

[25] X. Guo, Y. Zhan, C. Chen, B. Cai, Y. Wang, and S. Guo, "Influence of packing material characteristics on the performance of microbial fuel cells using petroleum refinery wastewater as fuel," *Renew. Energy*, vol. 87, pp. 437–444, 2016.

[26] A. Vilajeliu-Pons et al., "Microbiome characterization of MFCs used for the treatment of swine manure," *J. Hazard. Mater.*, vol. 288, pp. 60–68, 2015.
[27] B. E. Logan, "Exoelectrogenic bacteria that power microbial fuel cells," *Nat. Rev. Microbiol.*, vol. 7, pp. 375–381, 2009.
[28] M. J. Choi et al., "Effects of biofouling on ion transport through cation exchange membranes and microbial fuel cell performance," *Bioresour. Technol.*, vol. 102, no. 1, pp. 298–303, 2011.
[29] W. He, X. Zhang, J. Liu, X. Zhu, Y. Feng, and B. E. Logan, "Microbial fuel cells with an integrated spacer and separate anode and cathode modules," *Environ. Sci. Water Res. Technol.*, vol. 2, no. 1, pp. 186–195, 2016.
[30] A. E. Franks and K. P. Nevin, "Microbial fuel cells, a current review," *Energies*, vol. 3, no. 5, pp. 899–919, 2010.
[31] J. K. Jang et al., "Construction and operation of a novel mediator- and membrane-less microbial fuel cell," *Process Biochem.*, vol. 39, no. 8, pp. 1007–1012, 2004.
[32] A. Asghar, A. A. Abdul Raman, and W. M. A. Wan Daud, "Challenges and recommendations for using membranes in wastewater-based microbial fuel cells for in situ Fenton oxidation for textile wastewater treatment," *Rev. Chem. Eng.*, vol. 31, no. 1, pp. 45–67, 2015.
[33] L. Zhuang, S. Zhou, Y. Wang, C. Liu, and S. Geng, "Membrane-less cloth cathode assembly (CCA) for scalable microbial fuel cells," *Biosens. Bioelectron.*, vol. 24, no. 12, pp. 3652–3656, 2009.
[34] C. Santoro, C. Arbizzani, B. Erable, and I. Ieropoulos, "Microbial fuel cells: From fundamentals to applications. A review," *J. Power Sources*, vol. 356, pp. 225–244, 2017.
[35] M. Qin, E. A. Hynes, I. M. Abu-Reesh, and Z. He, "Ammonium removal from synthetic wastewater promoted by current generation and water flux in an osmotic microbial fuel cell," *J. Clean. Prod.*, vol. 149, pp. 856–862, 2017.
[36] M. Qin, Q. Ping, Y. Lu, I. M. Abu-Reesh, and Z. He, "Understanding electricity generation in osmotic microbial fuel cells through integrated experimental investigation and mathematical modeling," *Bioresour. Technol.*, vol. 195, pp. 194–201, 2015.
[37] R. M. Kadhim, E. E. Al-Abodi, and A. F. Al-Alawy, "Citrate-coated magnetite nanoparticles as osmotic agent in a forward osmosis process," *Desalin. Water Treat.*, vol. 115, pp. 45–52, 2018.
[38] F. A. Yaseen, A. F. Al-Alalawy, and A. Sharif, "Renewable energy by closed-loop pressure retarded osmosis using hollow fiber module," *AIP Conf. Proc.*, vol. 2213, no. March, 2020.
[39] M. Qin, I. M. Abu-Reesh, and Z. He, "Effects of current generation and electrolyte pH on reverse salt flux across thin film composite membrane in osmotic microbial fuel cells," *Water Res.*, vol. 105, pp. 583–590, 2016.
[40] I. Gajda et al., "Electro-osmotic-based catholyte production by Microbial Fuel Cells for carbon capture," *Water Res.*, vol. 86, pp. 1–8, 2015.
[41] Z. Ge, Q. Ping, L. Xiao, and Z. He, "Reducing effluent discharge and recovering bioenergy in an osmotic microbial fuel cell treating domestic wastewater," *Desalination*, vol. 312, pp. 52–59, 2013.
[42] H. A. Waheeb and A. F. Al-Alalawy, "Innovative microbial fuel cell design for investigation of cathode chamber effect and electricity generation enhancement," *AIP Conf. Proc.*, vol. 2213, no. March, 2020.
[43] S. Venkata Mohan, G. Mohanakrishna, S. Srikanth, and P. N. Sarma, "Harnessing of bioelectricity in microbial fuel cell (MFC) employing aerated cathode through anaerobic treatment of chemical wastewater using selectively enriched hydrogen producing mixed consortia," *Fuel*, vol. 87, no. 12, pp. 2667–2676, 2008.
[44] Y. Cao, Y. Hu, J. Sun, and B. Hou, "Explore various co-substrates for simultaneous electricity generation and Congo red degradation in air-cathode single-chamber microbial fuel cell," *Bioelectrochemistry*, vol. 79, no. 1, pp. 71–76, 2010.
[45] F. Zhang, K. S. Brastad, and Z. He, "Integrating forward osmosis into microbial fuel cells for wastewater treatment, water extraction and bioelectricity generation," *Environ. Sci. Technol.*, vol. 45, no. 15, pp. 6690–6696, 2011.
[46] J. Vilas Boas, V. B. Oliveira, L. R. C. Marcon, D. P. Pinto, M. Simões, and A. M. F. R. Pinto, "Effect of operating and design parameters on the performance of a microbial fuel cell with Lactobacillus pentosus," *Biochem. Eng. J.*, vol. 104, pp. 34–40, 2015.